ELSEVIER

Deep-Sea Research II 52 (2005) 495–512

DEEP-SEA RESEARCH
PART II

www.elsevier.com/locate/dsr2

Variability of Antarctic bottom water flow into the North Atlantic

Richard Limeburner*, J.A. Whitehead, Claudia Cenedese

Department of Physical Oceanography, Woods Hole Oceanographic Institution, Woods Hole, MA 02543, USA

Received 3 February 2004; accepted 8 December 2004

Abstract

The flow of Antarctic bottom water from the Brazil Basin in the South Atlantic into the Guiana Basin in the western North Atlantic has been measured by current meters for 44 months. Flow is confined by a relatively flat 4500-m-deep passage between 1°S and 4°N with complex sidewall shape. At the southern end is a 300-km-wide zonal channel straddling the equator between 32°W and 38°W with approximately a 500-m-deep layer of bottom water. The deep Antarctic bottom water current into the North Atlantic is confined to a region south of the equator and the direction is westward. Previous measurements of this deep current over 600 days in duration (J. Phys. Oceanogr. 27 (1997) 1903) indicated both a small warming trend and a decreasing volume flux. New data presented in this paper of 1388 days duration show no evidence for continuation of such trends. The average temperature and yearly averaged velocities are about the same as earlier at revisited locations. The long-term drift of the deep Antarctic bottom water temperature is about −0.002 °C/year and drift of the westward velocity is about 0.0015 m/s/year. The greatest variability is found near the top of the deep Antarctic bottom water at the northern edge of the current. The spectrum of the new 44-month data reveals a distinct yearly peak. We conclude that there has been no change in Antarctic bottom water flux into the North Atlantic during the past decade.

1. Introduction

During the past century, the overall circulation of the oceans has gradually become more clearly quantified through the use of a wide variety of measurements. In some cases, the documentation is even so precise that large data sets now exist with sufficient accuracy and resolution to reveal long-term (> years) deviations from a mean circulation. Typical data sets used are: sea surface temperature from large numbers of ship records, sea surface temperature from satellite-borne sensors, ocean temperatures obtained by vast numbers of expendable recorders (XBT's), precision altimetry from satellites, collections of all historical salinity–temperature records, long-term pressure records, including tide gauges, geostrophic

*Corresponding author.
E-mail address: rlimeburner@whoi.edu (R. Limeburner).

0967-0645/$ - see front matter © 2005 Elsevier Ltd. All rights reserved.
doi:10.1016/j.dsr2.2004.12.012

estimates of current flow, and current meter measurements of prominent currents. Data sets with sufficient coverage in space and time to find deviations from a mean apply mostly to circulation in the top half of the ocean, and some sets can even be used to aid meteorological forecasts (Goni and Trinanes, 2003). In contrast, the deep bottom half of the overturning circulation of the ocean has fewer data sets with sufficient coverage to indicate long-term (> years) temporal variations in circulation. This is unfortunate, since this deep circulation is significantly influenced by atmospheric climate variations, especially over time intervals longer than decades.

Our study is motivated by the desire to analyze one deep current long enough to detect slow changes with time of the deep ocean circulation. This includes interannual time scales and shorter term variability down to semidiurnal frequencies. The short-term variability on tidal frequencies is presented to provide data for model verification. The best candidates for finding significant mean flows with current meters are generally felt to be either along the Western boundary of the deep oceans (Warren, 1981), or in deep gaps between abyssal basins (Whitehead, 1998). A total of 20 long-time measurements now exist below 2000 m (Hogg, 2001).

Flows through gaps are particularly suitable for this purpose. Western boundary currents seem less desirable because they are subject to fluctuations of eddies passing by and offshore gyres may be active. In addition, there are already good examples of such measurements in gaps shallower than 1000 m. An excellent example above a ~650-m-deep gap is the "Denmark Strait overflow water" measured by Dickson and Brown (1994), who used 91 current meters downstream of the gap. They found a complete lack of seasonal variability in temperature, thickness, or speed. The current was so steady throughout the period of measurement that it was stated that measurements for a month would have sufficed as well as their measurements of more than a year. In contrast, another shallow flow has indications of slow changes. This flow is located at the ~900 m deep Faroe-Bank Channel between Scotland and the Faroe Islands. Water from the Greenland–Norwegian Sea passes through this gap and descends into the deep eastern North Atlantic southeast of Iceland. Although no long-term trend was found in measurements of this overflow by Saunders (1990), Hansen et al. (2001) present evidence of a gradual decrease of this flow from current meter measurements over a four year period from 1995 to 1999.

We felt that the deepest flow entering the western North Atlantic from the south, which involves the water mass commonly called Antarctic bottom water, was an excellent candidate for long-term monitoring. There have been extensive measurements of flows through deep gaps into and out of the Brazil Basin regions thanks to the Deep Basin Experiment of the World Ocean Circulation Experiment of the 1990s. The Brazil Basin lies in the Western Atlantic south of the equator. Water of Antarctic origin (frequently called Antarctic bottom water) enters the southern end of this basin at approximately 30°S through both the Vema Channel and the Hunter Channel, which lies further to the east. This water, which typically is defined as colder than 1.9 °C potential temperature, is found below depths of about 4000 m. Transport estimates of flow through the Vema channel using current meters are made by Hogg et al. (1982), Hogg and Zenk (1997), and Hogg et al. (1999), and are summarized by Hogg (2001). The flux is 4.0 Sv (throughout this paper we use the standard volumetric flow rate of $1\,\mathrm{Sv} = 10^6\,\mathrm{m}^3/\mathrm{s}$) with a standard deviation of ± 1.2 Sv. Based upon an integral time scale of 10 days the standard error is estimated at ± 0.2 Sv. Flux through the Hunter Channel about 2.9 ± 1.2 Sv (Zenk et al., 1999; Hogg et al., 1999). The flows in the center of the currents have a constant northward component with time-dependent fluctuations that are less than half the steady value. An earlier estimate of fluxes (Speer and Zenk, 1993) from hydrographic measurements gave the Vema channel flux at 3.9 Sv, which is very close to the value above. However the estimates of 2.0 Sv flux in the Western Boundary current upon the lower Santos Plateau and 0.7 Sv through the Hunter Channel were substantially different from the current meter results. Although the source of the differences between current meter results and geostrophic

estimates cannot be located with absolute certainly, at least some of the difference arises because current meter arrays give a time average that is not available to geostrophic estimates. Finally, there is an increase in temperature of about 0.02 °C in the coldest water within the Vema Channel (Zenk and Hogg, 1996; Hogg and Zenk, 1997; Hogg, 2001). Further south, in the Argentine Basin, a similar size of warming has also been found (Coles et al., 1996).

The Antarctic bottom water leaves the Brazil Basin in the north through a number of passages. The flow through the mid-Atlantic Ridge is found in the Romanche and Chain Fracture Zones, where it enters the Eastern Equatorial Atlantic. Mercier and Speer (1998) estimated the flux through the latter two passages to be 1.22 Sv, with a standard deviation of ±0.25 and standard error or ±0.04 (Hogg, 2001). The flow of interest in this paper is located in the Ceara Abyssal Plain, which is a relatively flat region at a depth of about 4500 m between approximately 1°S, 34°W and 4°N, 40°W. The shape of the sidewalls makes this a rather tortuous path, with the water required to travel toward the west at the southern end, then perhaps northward between the equator and about 3°N, and then westward and north through rough gaps east of the Ceara rise and into the Guiana Basin. Early estimates of the flux of this water into the western North Atlantic did not agree. They varied from a low of 1.0 or 2.0 Sv (Whitehead and Worthington, 1982) up to 4.0 Sv (Luyten et al., 1993; McCartney and Curry, 1993). In spite of the different estimates of the magnitude of the volume flux, there was little question about the persistence of the current. These considerations motivated Hall et al. (1997) to measure the flux within the layer of Antarctic bottom water at the southern end of the Ceara Abyssal Plain in an east–west trending channel between 34° and 40°W as shown in Fig. 1. This gap straddles the equator from about 1°30′S to 1°N and is approximately 4500 m deep. The 6-mooring array was located along a north–south line at 36°W with current meter depths ranging from 3000 m to just above the bottom. The roughly 600 day long current meter and temperature records from September 1992 to June 1994 revealed a westward flow in the portion

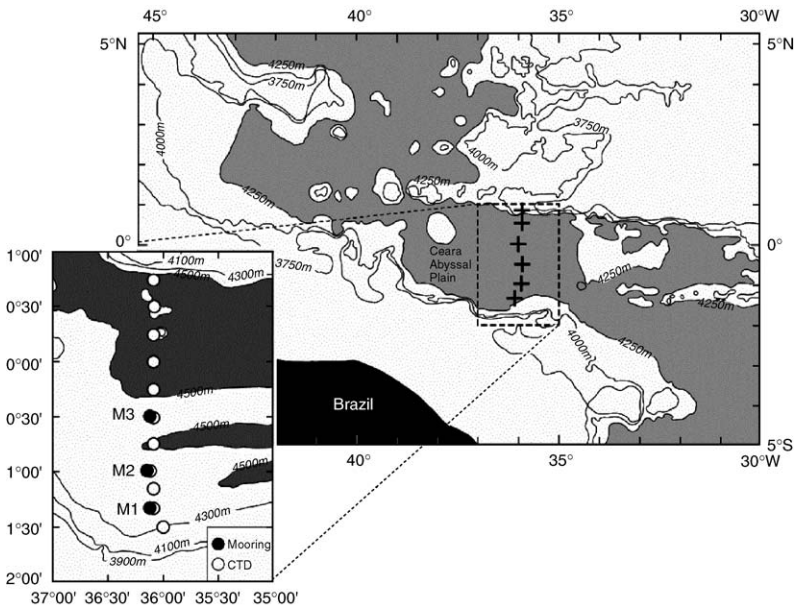

Fig. 1. The large map shows the 3750, 4000, and 4250-m contours that define the channel over the Ceara Abyssal Plain between the western portions of the North and South Atlantic. The pluses show the location of current meters by Hall et al. (1997). The inset shows the location of CTD stations (open circles) and moorings (solid circles) during 1999–2003.

of the channel below about 4000 m. This deep current is about 500-m thick and it is found only in the portion of the channel south of about 0°15′S. It had a mean speed of about 0.05 m/s. A larger current in the opposite direction lay above 4000 m in the Lower North Atlantic Deep Water. The shape of the sidewalls is such that the westward flowing Antarctic bottom water enters the North Atlantic through a route over the Ceara Abyssal Plain, which remains at roughly 4500 m depth up to about 4°N. The mean flux of bottom water from the aggregate current meter data was estimated to be about 2.0 Sv. Fluctuations were abundant, but they produced a standard deviation of only about 0.9 Sv, so they did not overwhelm the mean flow. There were prominent fluctuations at roughly a 120-day period and at other periods including yearly as well. The measurements also agreed with estimates of instantaneous flux by Rhein et al. (1995, 1998) of 2.6 Sv based upon lowered current meters.

Filtering the time-dependent signals revealed a slow decrease in the yearly mean value, with about a 10% decrease in transport between the first year's average and the average of the last year of the record. We estimate here that the drift is the same size as a standard error of 0.2 Sv based upon the above standard deviation, a 120-day fluctuation, and a 600-day record. Thus the decrease is only marginally statistically significant. However, the decreased flow was also associated with a clear 25–40-m descent of all isotherms for potential temperature $<1.8\,^{\circ}C$. This descent has also been described as a warming of the water. However, the very deepest water exhibited much smaller warming than the water in the "benthic thermocline" which is a sharp transition region between Antarctic bottom water and North Atlantic deep water that lies above it. This transition is found near the bottom at depths of 4000–4200 m. This layer of sharp temperature change signifies transition from Antarctic bottom water (below) to Lower North Atlantic deep water (above). The descent of the isotherms produced changes in temperature at a fixed level of 0.098 °C/year at 4100 m and 0.016 °C/year at 4300 m so that temperature change was not uniform throughout the water column. Thus "descent of the isotherms" is more accurate than "warming."

2. Hydrography and moored array results

2.1. Mooring design

In order to optimize the comparison between measurements in the new project and the data gathered by Hall et al. (1997) three mooring locations were reoccupied along a north–south line at about 36°05′W at approximately 1°20′S, 1°00′S, and 0°30′S as shown by the inset in Fig. 1. These were called M1, M2 and M3 from south to north. After 22 months the current meters were replaced for about another 22-month period. Thus each mooring name is followed by a second number indicating first or second deployment. The exact locations, durations, and bottom depths are shown given in Table 1 and discussed below. In addition, CTD casts were taken at and between each mooring, and also south of the southern mooring on the first cruise and north to the equator as well. Six VACM current meters and 6 Sea Bird Temperature Recorders were deployed during the fieldwork. With three current meters we reoccupied the three 4300-m-deep current meter locations in the core of the current made by Hall et al. (1997). In order to get even better data than before, three additional current meters were located at a level of 4200-m depth. We felt that placing current meters at 4200-m depth was superior to reoccupying the 4100-m level used earlier, because the old levels had clearly been influenced by the intense shear between this current and the current going in the opposite direction above it.

Locating the current meters at exact depths was a priority. Care was taken to determine the bathymetric depth at the mooring site and to locate the current meters as close as possible to the desired depths. To this end, the moorings were designed to be deployed in the depth of the previous mooring and upon arrival at the site the bathymetric depth below the ship was determined as accurately as possible by using sound speed corrections from the CTD data. Then wire lengths

Table 1
Mooring deployments and recoveries, and CTD station locations, times, and bottom depths

Station	Date	Time UTC	Latitude (S)	Longitude (W)	Depth (m)
CTD 11	4/4/99	1157	1°30.2350′	35°59.5483′	4271
Deploy M11	4/4/99	2130	1°19.9307′	36°05.2472′	4439
CTD 12	4/4/99	2217	1°19.8117′	36°05.0933′	4439
CTD 13	4/5/99	0225	1°09.9900′	36°04.9983′	4340
Deploy M21	4/5/99	1139	0°59.2200′	36°07.2124′	4417
CTD 14	4/5/99	1152	0°59.5387′	36°06.9300′	4411
CTD 15	4/5/99	1634	0°45.1000′	36°04.9850′	4451
Deploy M31	4/5/99	2311	0°30.2940′	36°05.8460′	4484
CTD 16	4/5/99	2330	0°30.4217′	36°05.4533′	4481
CTD 17	4/6/99	0459	0°15.0667′	36°04.9800′	4518
CTD 18	4/6/99	0920	0°00.0300′N	36°4.9383′	4504
Recover M31	2/23/01	1855	00°30.250′	36°06.020′	
CTD 26	2/23/01	2104	00°30.260′	36°06.090′	4494
Deploy M32	2/24/01	0216	00°30.299′	36°05.844′	4493
CTD 25	2/24/01	0500	00°44.820′	36°06.080′	4475
Recover M21	2/24/01	0942	00°59.920′	36°06.110′	
CTD 24	2/24/01	1131	00°59.940′	36°07.270′	4425
Deploy M22	2/24/01	1920	00°59.203′	36°07.234′	4427
CTD 23	2/25/01	0206	01°09.739′	36°06.185′	4421
Recover M11	2/25/01	0820	01°20.000′	36°05.240′	
CTD 22	2/25/01	1010	01°19.578′	36°05.562′	4449
Deploy M12	2/25/01	1642	01°19.931′	36°05.254′	4448
CTD 262	2/26/01	0548	00°30.900′	36°06.060′	4496
CTD 27	2/26/01	1015	00°14.961′	36°05.874′	4525
CTD 28	2/26/01	1430	00°00.008′	36°05.780′	4529
CTD 32	1/21/03	0904	01°20.48′	36°05.927′	4443
Recover M12	1/21/03	1206	01°19.92′	36°05.27′	
CTD 34	1/21/03	1645	01°00.09′	36°07.13′	4390
Recover M22	1/21/03	1933	00°59.22′	36°07.48′	
CTD 36	1/22/03	0045	00°30.12′	36°05.64′	4475
Recover M32	1/22/03	0846	00°30.33′	36°05.94′	
CTD 38	1/22/03	1441	00°00.08′	36°04.84′	4514
CTD 37	1/22/03	1913	00°14.91′	36°04.88′	4506
CTD 35	1/23/03	0128	00°44.97′	36°04.95′	4446
CTD 33	1/23/03	1630	01°10.01′	36°05.05′	4364

The moorings are designated by "M" followed by two integers. The first integer indicates whether the mooring was at the southern (M1), middle (M2), or northern (M3) end of the array. The second integer denotes whether it was the first or second mooring deployed at that location. The CTD stations are designated by "CTD" followed by two integers. The first integer indicates whether the CTD station was made during the first, second, or third cruise, and the second denotes the sequence in time during each cruise.

were revised as needed. The depths are listed in Table 2 in the next section. We estimate that the depths of the current meters are accurate to better than 3 m.

The moorings were designed to measure the velocity and temperature over a 2-year period. Each mooring consisted of an EG&G BACS acoustic release, Sea Bird Electronics temperature recorders located 50 and 150 m off the bottom sampling every 7.5 min, VACM/T recorders located 100 and 200 m off the bottom vector averaging every 30 min, and glass flotation balls for buoyancy. A simple schematic of the mooring design is shown in Fig. 2.

In order to resolve the effects of time-dependent currents, it was necessary to make these measurements for as long a time as possible. Therefore, these records are comprised of current meter

Table 2
Depths of the current meters and temperature sensors

Mooring	1999–2001 Depth (m)	2001–2003 Depth (m)
M3-VACM	4191	4197
M3-TR	4241	4246
M3-VACM	4291	Failed
M3-TR	4304	4347
M2-VACM	4218	4218
M2-TR	4268	4267
M2-VACM	4317	4317
M2-TR	4367	4367
M1-VACM	4214	4197
M1-TR	4264	4246
M1-VACM	4314	4297
M1-TR	4363	4347

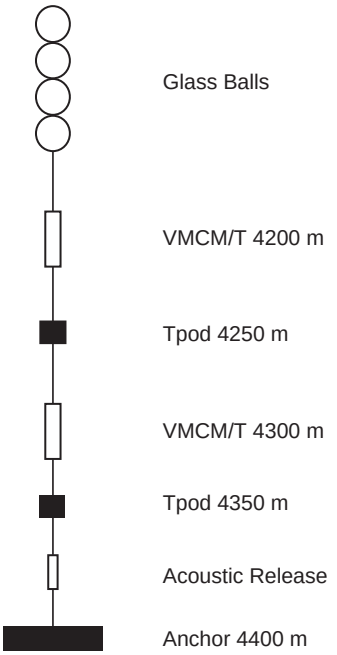

Fig. 2. The subsurface mooring design. The shown depths are nominal only. The final depths are listed in Table 2.

measurements, each about 22 months long. Five current meter locations had a pair of such sequential measurements. Unfortunately, the sixth current meter location only has one 22-month-long record due to damage of one current meter.

Three cruises were employed to deploy and recover the two sets of moorings. As much as possible, the CTD stations, and of course the mooring locations, are located along the same line and at the same locations as those occupied by Hall et al. (1997). On April 3, 1999, the R/V *Seward Johnson* (Cruise SJ9903) departed Natal, Brazil and steamed north to 2°00′S, 36°05′W, the southern edge of the deep equatorial channel. The first CTD station was located just outside of Brazilian territorial waters and was begun on April 4, 1999. That same day, the site of mooring M1 was approached and the mooring was launched, after which a second CTD station was taken close to that location. Then a third CTD was taken midway between the sites of M1 and M2. The sequence was repeated for mooring M2 and M3 and CTD stations were made every 15′ up to 0°45′N. A similar procedure was made for recovery and redeployment of a second set of moorings, and CTD locations were only taken as far north as the equator for the last cruise. On the first recovery cruise, the deployment of the second set of moorings was completed, and another set of CTD casts was made on the R/V *Oceanus* (Cruise OC 365-3) that departed February 16, 2001 from Bridgetown, Barbados. The recovery of the second set of moorings and a third set of CTD casts was taken on the final cruise on R/V *Oceanus* (Cruise OC 385-3) that departed Fortaleza, Brazil on January 20, 2003.

Table 2 lists the final depths of the temperature and velocity sensors. The depths were determined using sonar depth corrections for the speed of sound using the hydrographic casts and checking the final depths between CTD data and temperatures on the moored recorders whenever possible.

2.2. The hydrographic and moored temperature data

Hydrographic data from the CTD stations were used to produce a potential temperature section along a constant longitude line at approximately 36°05′W between 0°45′N and 1°20′S encompassing the whole width of the channel connecting the Brazil Basin in the South Atlantic and the Guiana Basin in the North Atlantic. We considered data

from our three cruises and compared those to the data from the two cruises of Hall et al. (1997), the first one in 1992 on R/V *Iselin* and the second one in 1994 on R/V *Knorr*. Fig. 3 illustrates the five potential temperature sections. Since flow above 3800 m is not a topic of the present study, the section is shown only between the ocean bottom and 3800 m. Other transits had small differences in bathymetry, but no substantial differences. The Antarctic bottom water is usually defined as water colder than 1.8 °C (Hall et al., 1997) or 1.9 °C (Whitehead and Worthington, 1982) and from Fig. 3 it is obvious that the transition between the Antarctic bottom water and the overlying lower North Atlantic deep water is represented by the strong temperature gradient lying between 4100 and 4300 m.

In order to investigate the change of the depth of the transition region with time we show in Fig. 4 the depths of the 1.8 °C, 1.4 °C, and 1.0 °C isotherms for the 5 different cruises. Fig. 6 of Hall et al. (1997) shows a larger moored temperature

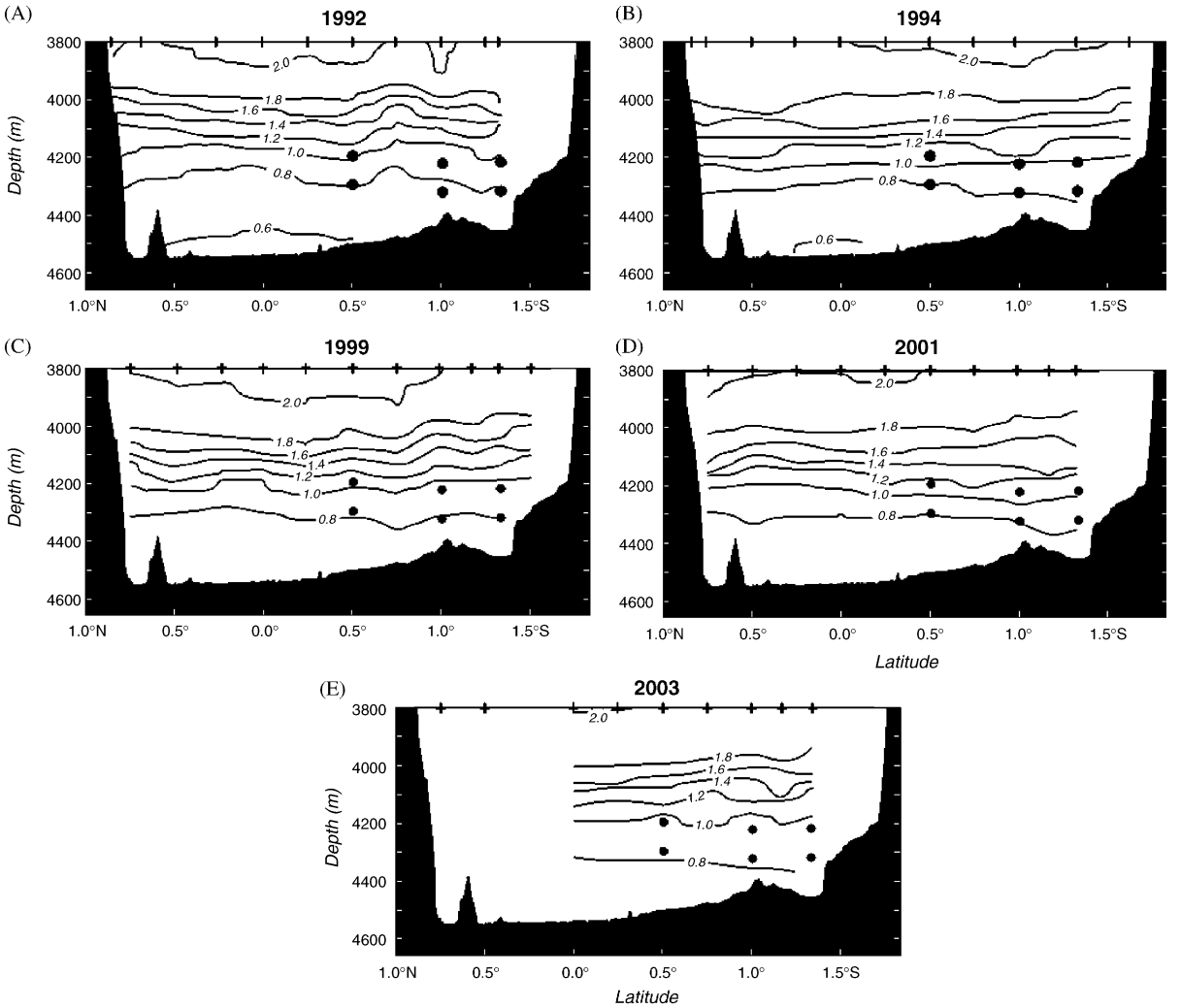

Fig. 3. Potential temperature sections from (respectively left to right and top to bottom) (A) *Iselin* 1992, (B) *Knorr* 1994, (C) *Seward Johnson* 1999, (D) *Oceanus* 2001 and (E) *Oceanus* 2003. The crosses at the top of the figures denote the CTD locations. In each of the panels, the black solid circles represent current meter locations and the bathymetry (collected in 2001) is the same for all panels.

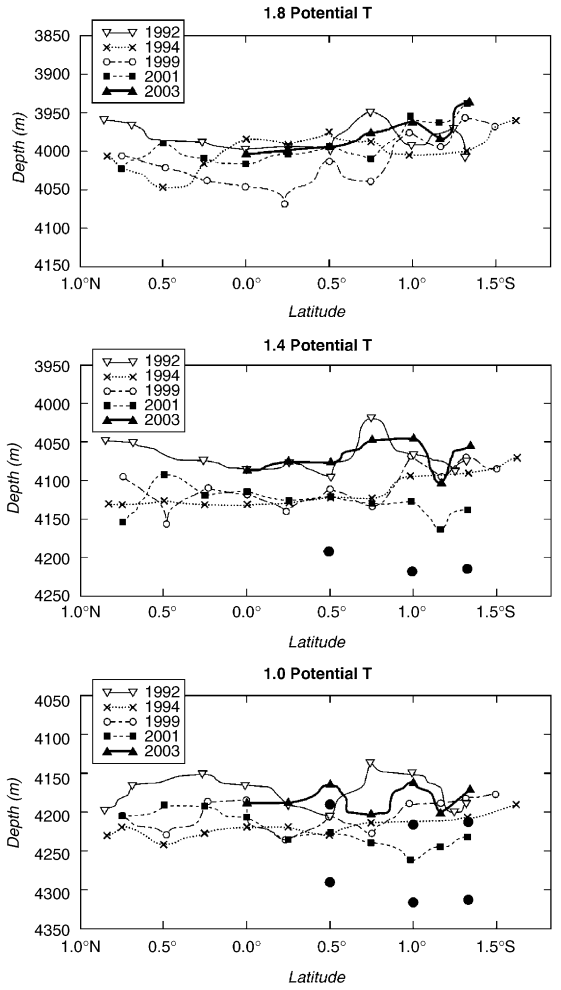

Fig. 4. Depth of the 1.8 °C, 1.4 °C, and 1.0 °C potential temperature (Potential T) isotherms for the five sections. Current meter locations are shown as solid circles.

change with time at the equator at 4093 m and a weaker temperature change at 4292 m, while moored temperature below 4292 m and above 4093 m do not show significant changes in temperature. This is not surprising if we consider that the vertical movement of the transition layer with the high temperature gradients leads to stronger temperature variability when compared to regions where the vertical temperature gradient is weak. In Fig. 4 one can observe the above-mentioned vertical displacement of the 1.8 °C, 1.4 °C, and 1.0 °C isotherms at the equator between 1992 and 1994. However, such vertical displacement is present between −1°S and 1°N, but is less pronounced or absent between −1°20′S and −1°00′S. Furthermore, the isotherms for the following 3 years (1999, 2001, and 2003) show that the warming trend observed by Hall et al. (1997) of 0.098 °C/year, which corresponds to an isotherm deepening of 40 m at 4100 m, did not persist. Instead, each of the isotherm depths shown in Fig. 4 presents a variability both in space, along the section, and in time, between 1999 and 2003, of approximately the same amount (±60 m) as observed between 1992 and 1994.

Table 3 shows some of the simple statistics for the moored data obtained at the three mooring sites. The temperature standard deviation for the aggregate data set is ±0.066 °C, which corresponds approximately to a ±30-m vertical displacement of isotherms. This is about the size of the standard deviations of all the points in each panel of Fig. 4, of which top to bottom are 28, 33, and 28 m.

Table 3
Statistics of the current meter data

Mooring Nominal Depth (m) 1999–2003	$\langle u \rangle$ (m/s)	$\langle v \rangle$ (m/s)	$\sqrt{\langle u'^2 \rangle}$ (m/s)	$\sqrt{\langle v'^2 \rangle}$ (m/s)	$\sqrt{\langle u'v' \rangle}$ (m/s)	$\langle T \rangle$ (°C)	$\sqrt{\langle T'^2 \rangle}$ (°C)	$\langle u \rangle$ (m/s) 1992–1994	$\langle v \rangle$ (m/s) 1992–1994
M3-4200	−0.078	0.010	0.055	0.034	−0.075	1.37	0.076		
M3-4300	−0.051	0.007	0.036	0.030	−0.015	1.15	0.031	−0.0422	0.0032
M2-4200	−0.035	0.004	0.035	0.041	0.032	1.33	0.067		
M2-4300	−0.011	0.002	0.027	0.033	0.015	1.16	0.034	−0.0135	0.0002
M1-4200	−0.058	−0.005	0.047	0.033	0.037	1.35	0.055		
M1-4300	−0.055	−0.003	0.041	0.029	0.025	1.23	0.037	−0.0488	−0.0042

Each record was 1387 days long except for M3-4300, which was 689 days long. Brackets denote an average over the entire length of the record.

This variability can be also clearly observed by looking at the moored temperature time series. The two 2-year moored current meter and temperature data sets were merged together and interpolated to a common one-hour time base to linearly fill the approximate 8–10-h gaps between recovering the first deployment and redeploying the second deployment. This results in approximately 4-year records of velocity and temperature at each mooring site. The M1 hourly temperature data is shown in Fig. 5. The deepest temperature record was short due to instrument failure.

The temperature variability on time scales of days at M1 was typically about $\pm 0.06\,^{\circ}C$ and this corresponds approximately to a ± 30 m vertical displacement of isotherms so the isotherm depth for each of the cruises in Fig. 4 needs to be interpreted with caution. Fig. 5 also shows the relatively small range of the temperature variability of the Antarctic bottom water.

Fig. 6 shows the temperature time series for 11 sensors from all the 1999–2003 moorings with a 365 days box filter (running mean). The slope of a least squares fit to all of 8 data sets that run for the full time period is $-0.002\,^{\circ}C$/year and the thick black line shows this trend. The trend is slightly cooling. Thus, no warming trend is observed and variability is of order of $-0.002\,^{\circ}C$/year and not of order $0.1\,^{\circ}C$/year as was previously observed at the equator at 4100 m for 1992–1994 data (Hall et al., 1997).

Hence we conclude that, although the deepening of the $1.0\,^{\circ}C$, $1.4\,^{\circ}C$ and $1.8\,^{\circ}C$ potential temperature isotherms between 1992 and 1994 indicated a warming trend between those 2 years, the trend was not observed in the following years in which measurements were taken. Instead, the depth of isotherms varied both spatially and in time and, as confirmed by the mooring time series, the temperature during 1999–2003 was fairly constant and no further trends were observed.

In summary within 11 years between 1992 and 2003 the AABW has been observed to undergo a warming trend between 1992 and 1994 (Hall et al., 1997) and to maintain a constant temperature between 1999 and 2003. This study leads us to the conclusion that the cold Antarctic bottom water does not seem to be warming in spite of changes up

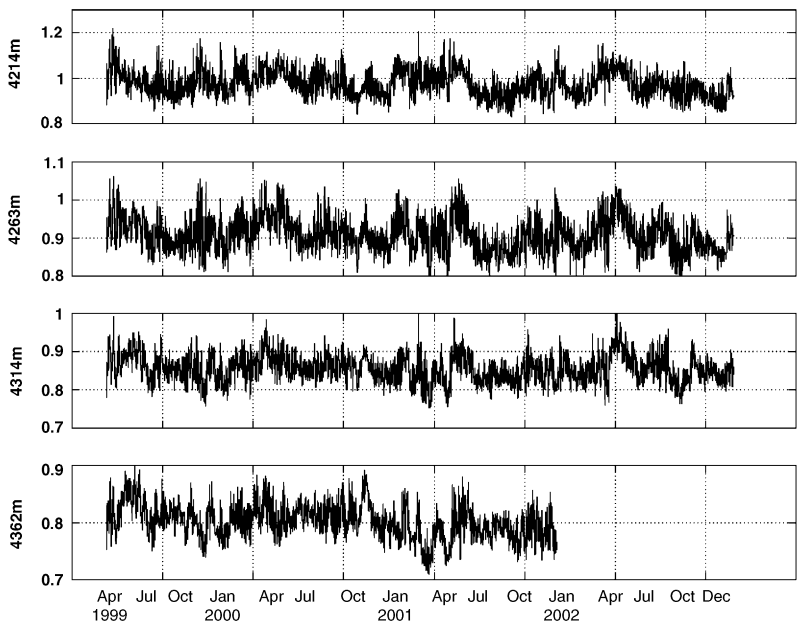

Fig. 5. M1 hourly potential temperature time series during the 4 years of deployment. The 10-h gap between deployments was filled by linear interpolation.

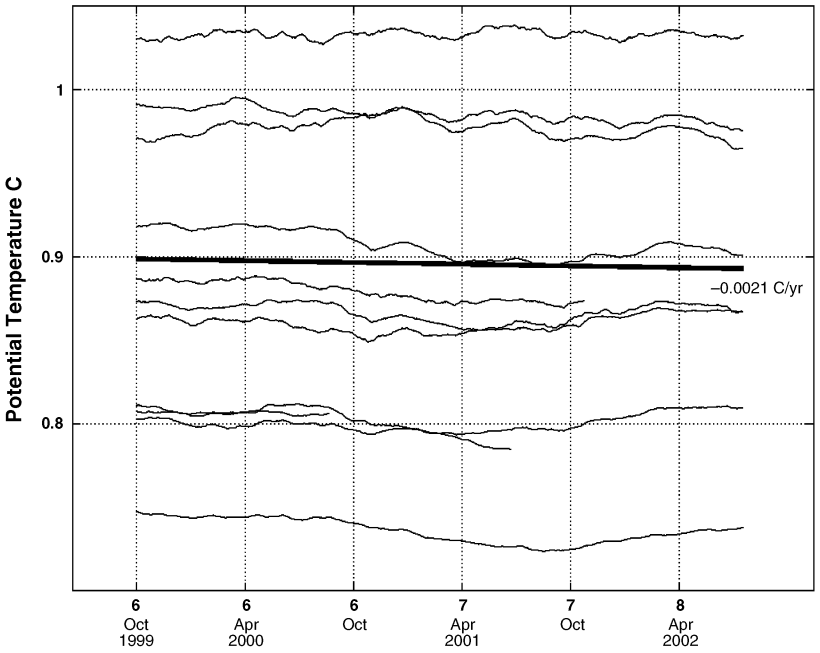

Fig. 6. All the moored temperature data smoothed with a 365-day running mean.

and down of potential temperature depths with time.

2.3. Moored current meter data

The current meter data return was generally good except for the failure of the current meter at a depth of 4300 m at the M3 mooring during 2001–2003. Each other instrument collected data of speed, direction and temperature over 600 days. Some statistics of the current meter data are listed in Table 3. A time series of 30-min east velocity raw data is shown for the first 100 days of the 1999 deployment in Fig. 7 for all the current meter data. Westward current was plotted as negative values. The tidal contribution is readily visible as a small oscillation with about 0.05 m/s amplitude with a semidiurnal period. See Appendix A for a summary of the tidal constituents from all the current meter data. The northward component (not shown) varies by about 0.05 m/s about zero. The eastward component has two typical types of flow during the first 100 days of the deployment. One has a weakly westward current with speeds of less than 0.05 m/s. The other has more frequent intervals of westward flow with speed between −0.05 and −0.2 m/s.

The M1 low-pass-filtered east velocity at a depth of approximately 4314 m is shown in Fig. 8 for a period of 1383 days (3.8 years), April 6, 1999 to January 18, 2003. Westward current was plotted as negative values. The hourly east velocity plotted in Fig. 8 was low-pass-filtered to remove tidal and high-frequency oscillations with periods less than 10 days (Beardsley et al., 1985). The data from this mooring location and depth had temperatures most characteristic of AABW compared to the other measurements at all the moorings. The 4-year M1 mean east velocity at 4310 m was −0.06 m/s with a maximum of 0.03 m/s and a minimum of −0.19 m/s. The mean north velocity was −0.003 m/s with a maximum of 0.12 m/s and a minimum of −0.13 cm/s. Thus the westward zonal current dominated the mean velocity. The strongest flow to the west was over periods of about 10 days during June 1999, November 1999, and June

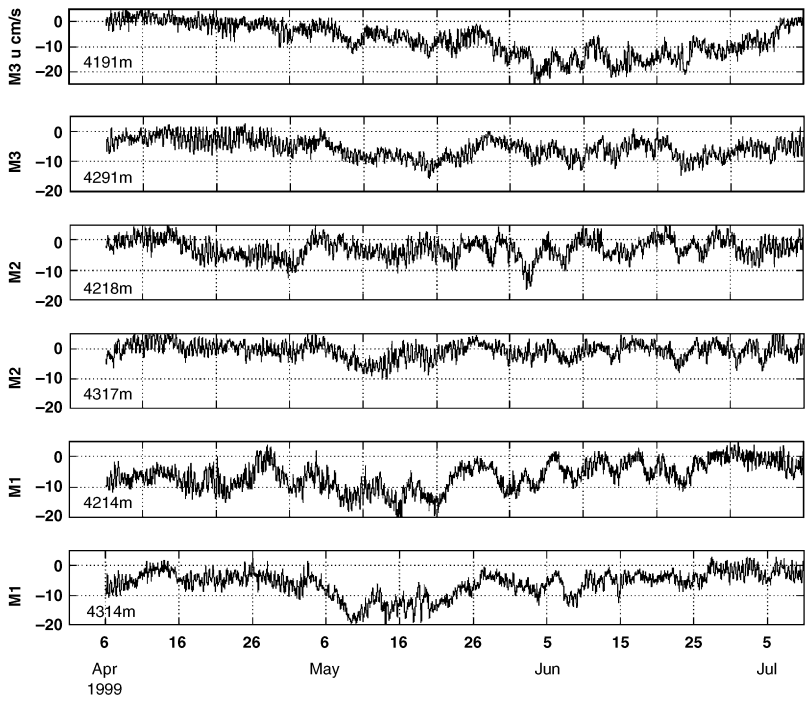

Fig. 7. Time series of 30-min east velocity data for the first 100 days of 1999. Westward currents were plotted as negative values.

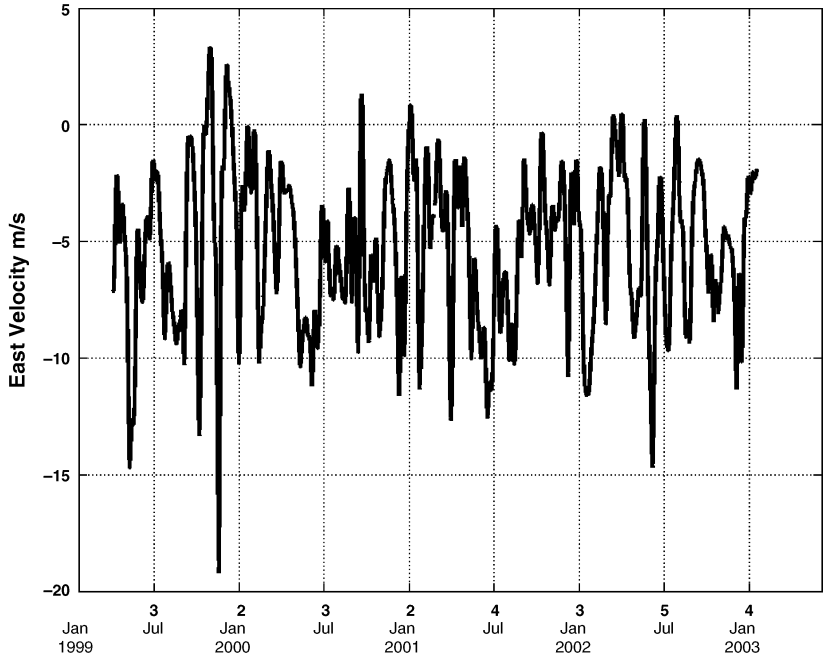

Fig. 8. The M1 east velocity at a depth of approximately 4314 m for a period of 1383 days (3.8 years), April 6, 1999 to January 18, 2003. Westward current was plotted as negative values. The data were low-pass-filtered to remove tidal and high-frequency oscillations with periods less than 10 days.

2002. The greatest fluctuations occurred in 1999. There appears to be an annual signal in the east velocity during the first 2 years, but not in the last 2 years and strong variability of the westward current in Fig. 5 is observed at about 50 days.

The kinetic energy spectrum for the M1 mooring hourly east velocity at a depth of 4314 m is shown in Fig. 9. The current meter data from all the moorings was generally not coherent nor in phase but the data shown in Fig. 9 is representative of the variability at the other instrument locations. The spectrum in Fig. 9 exhibits clear peaks in the diurnal and semidiurnal bands that are more than one order of magnitude less that the observed peaks at lower frequencies. A spectral peak is observed at 51 days with equal contributions of the clockwise and counterclockwise components indicating a one-dimensional oscillation in the zonal direction. The mostly counterclockwise spectral peak at 59 days indicates the variability was more elliptical at this frequency (see Stammer and Boning, 1992). The peak at 197 days was dominated by counter clockwise energy, and the clockwise peak at 348 days had the highest energy density.

3. Discussion

3.1. Interpretation of the time records

The statistics of the current meter data are shown in Table 3. For comparison, the mean flow of 1992–1994 data for the co-located current meters at about 4300 m depth is also shown in Table 3.

Fig. 10 shows the east velocity time series for the 6 current meters from all the 1999–2003 moorings with a 365 days box filter (running mean). The slope of a least squares fit to all of the 5 data sets

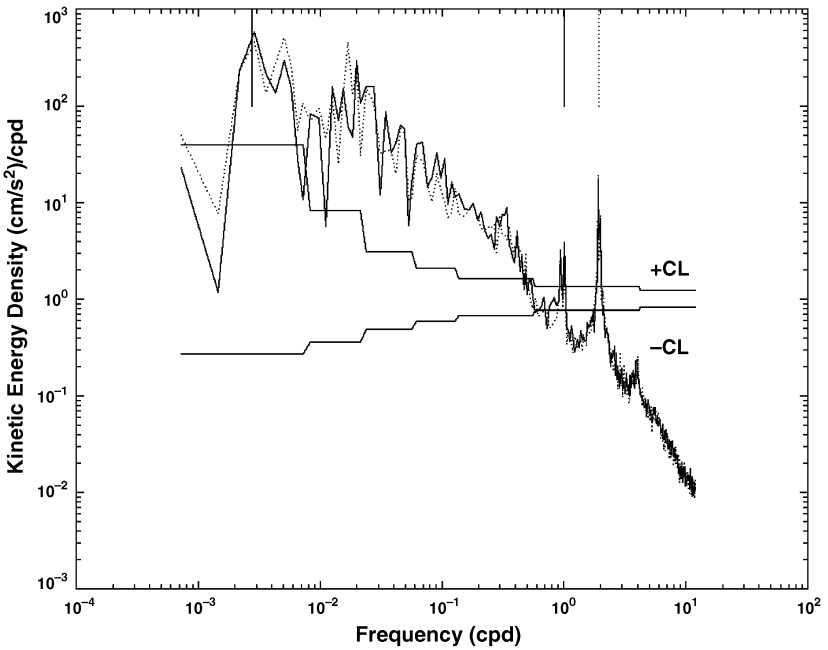

Fig. 9. Mooring M1 rotary kinetic energy spectrum at a depth of 4314 m for a period of 1383 days (3.8 years) April 6, 1999 to January 18, 2003. The counterclockwise (CCW) and clockwise (CW) components are denoted by solid and dashed curves. A dashed vertical line shows the center of the semidiurnal band (12.4 h) and solid vertical lines show the center of the diurnal (24 h) and annual band (365 day). The 95% confidence limits are plotted along the bottom for reference. The upper and lower confidence limits are also shown. The CCW and CW components of the energy are denoted by solid and dashed curves.

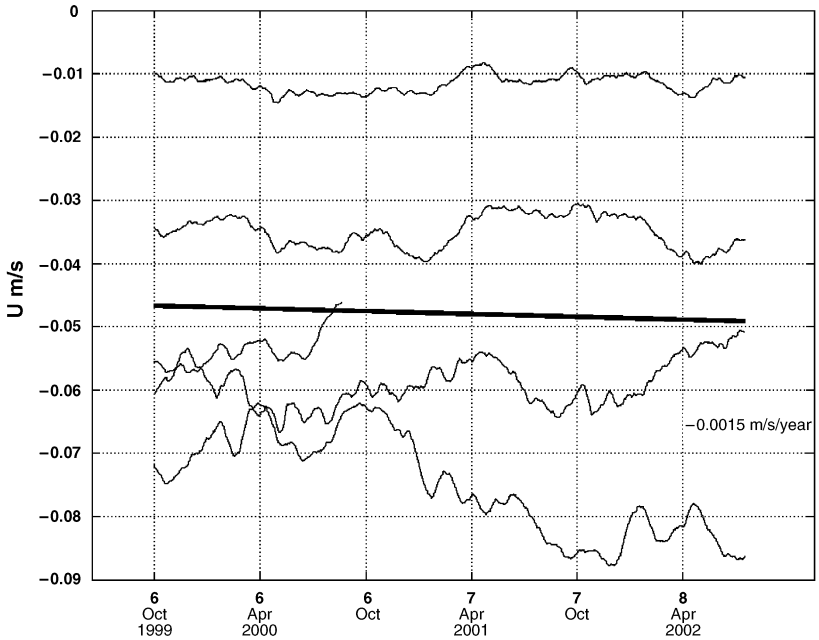

Fig. 10. The 365-day running mean eastward velocity of all the current meter data. The straight line is the least-squares fit to the five long records. The data records are top to bottom: M2-4300, M2-4200, M3-4300, M1-4300, M1-4200 and M3-4200.

that run for the full time period is −0.0015 m/s/year and the thick black line shows this trend. This indicates slightly increasing westward currents, although the trend is dominated by only one current meter (M3-4200). In summary, no decreased transport trend is observed and variability is of order of 0.005 m/s.

Since the purpose of this study is to compare the westward component of the flow with the earlier measurements, the speed of the westward flow from one new current meter sequence and from one record of Hall et al. (1997) is shown next. Fig. 11 shows this east velocity for the M1 mooring at 4314 m during the 1992–1994 period and also the 1999–2003 period. This record generally characterizes the data at the other locations. Also shown is a least squares fit to the data. There is very little decrease in the east velocity during 1999–2003 and the mean velocities of the new measurements are very close to the value of the earlier measurements. There is also little evidence for a decrease in east velocity with time in Fig. 11.

3.2. Estimation of volume flux

We do not have enough current meters to estimate volume flux directly, but at least two things indicate that the flux in the earlier period was about the same as the present flux. First, we note the compellingly close values of mean eastward velocity in Table 3 for the current meters in the repeat locations. Second the mean velocity in Fig. 10 along with an estimate of the area of the present current is in accord with the flux reported earlier. We illustrate this by assigning an area to the present array. Note that if one takes the vertical extent of the current flux to lie between the elevation of the 1.8 °C potential temperature and the bottom, the average layer thickness is about 400 m. This agrees with measurements of the vertical extent of the current by the moored array by Hall et al. (1997) and also by lowered Pegasus and ADCP data at two different times by Rhein et al. (1995, 1998). In addition the current meters indicate that the current starts south of the equator at about 0.25°S and extends to the

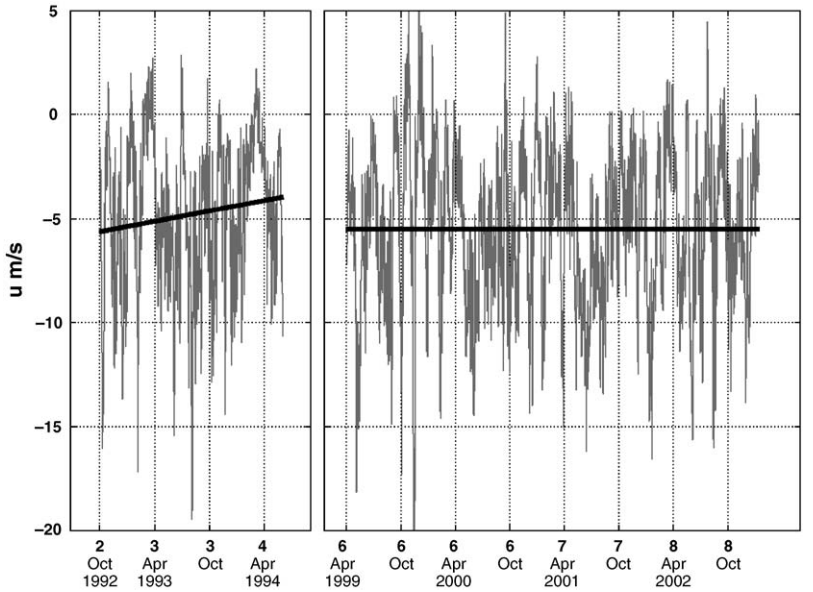

Fig. 11. Left, the M1 east velocity at a depth of 4314 m for a period of 609 days (1.67 years) October 2, 1992 to June 3, 1994 (Hall et al., 1997) and right, new data collected from April 4, 1999 to January 21, 2003. The east velocity data were low-pass-filtered with a 33-h cutoff and plotted in gray and a linear least-squares fit to the data was plotted as a solid black line.

southern wall at about 1.3°S. Therefore, we assign the width of the current to be about 100 km. Thus the area of the current across the passage is $4 \times 10^7\,m^2$. Using the Hall et al. (1997) reported average volume flux of 2.0 Sv, the average velocity is about 0.05 m/s. This number is just 5% more than the average of 4.74 shown by the midpoint of the line in Fig. 10.

We therefore assign an average volume flux of 2.0 Sv to the present data set, and in that case, the slope in Fig. 10 is equivalent to an increase of westward flux of 0.06 Sv/year, which is negligible. Moreover, it has the opposite sign from the decrease of about 0.3 Sv/year that is in the shorter 2 year record in Fig. 9 of Hall et al. (1997). Since mean eastward velocities in the repeat stations agree so closely, and since the longer data set shows such a small decrease, we conclude that for all practical purposes the flux is constant and changes are not likely to exceed 0.06 Sv/year which is about 3% per year. This has the same magnitude of slope as given by connecting old and new mean velocities with a straight line and finding its slope for two of the three repeat stations in Table 3. Over the time interval between the old and new records, the southern repeat mooring exhibited a 1.7% increase of speed per year to the west, the middle mooring exhibited a 3% decrease in speed, and the northern mooring exhibited a 3% increase.

4. Conclusion

There is little evidence that either the depth of the upper boundary of the Antarctic bottom water layer is descending or that the speed of the water flowing toward the west, and therefore into the North Atlantic is becoming significantly slower although changes on the order of 3% per year up and down are indicated at present. This applies to comparison of data sets between 1992–1994 with the sets of 1999–2003, and is also true of trends in recent moored thermometer and current meter data, which have records approximately twice as long as the earlier ones.

The trend in the deepening of the 1.8 °C, 1.4 °C and 1.0 °C isotherms found in 1992–1994 did not persist in the new data. Isotherms were scattered at different mean depths. In addition, the five sections from both research projects showed

variability with first a deepening of the isotherms in 1992–1994, then a shallowing in 1999 and a deepening again in 2001. Moreover, the spatial and temporal variability shown in Table 3 indicates that the typical temperature variability on the M1 mooring at 4314-m depth was about $\pm 0.05\,^{\circ}C$. Data from the vertical CTD temperature profiles can be used to find an equivalent typical vertical excursion of the isotherms and this comes to about ± 25 m. This range is about the same as the standard deviation of isotherm depths shown in Fig. 4 for five sections of about ± 30 m.

The 1992–1994 data had little long-term drift of temperature with time except for temperature at about $1.6\,^{\circ}C$, which was in the middle to the transition layer between Antarctic bottom water and North Atlantic deep water. This temperature drifted upward by about $0.2\,^{\circ}C$ over the two years of data collection with an equivalent rate of $0.1\,^{\circ}C$/year. No such trend was found in the new data collected during 1999–2003 where temperatures on average became colder at a rate of about $0.002\,^{\circ}C$/year.

Clearly for the 1361 days that the current was measured during 1999–2003 the westward flow was evident most of the time with each current meter. The mean temperature varied by $\pm 0.01\,^{\circ}C$ and velocity by ± 0.08 m/s and these fluctuations were of the same order of magnitude as the mean. These values are very similar to those in the earlier records. The strength of the mean current during 1999–2003 was within about 20% of the strength of current measured in 1992–1994 at the current meters deliberately placed in the same locations at about 4300 m. As shown in Table 3, at the northern mooring the 1992–1994 eastward mean velocity was -0.040 m/s and the 1999–2001 velocity was -0.050 m/s, which is a 21% increase. At the middle mooring the 1992–1994 mean eastward velocity was -0.014 m/s and the 1999–2003 mean velocity was -0.011, which is a 20% decrease. In the southern mooring the 1992–1994 mean eastward velocity was -0.049 m/s and the 1999–2003 mean velocity was -0.055, which is a 13% increase. The northern components of the velocity vector had changes of about the same sizes, but the percentage change is relatively larger, of order of 100% because their means are much smaller. This is consistent with these changes being due to eddies rather than meanders of the current. In spite of this, the small percentage changes for two long data sets separated by about 10 years are remarkable. They not only attest to the accuracy and ruggedness of the instruments, but they also show that the current itself can be regarded as a permanent feature of the deep advection of a major water type into the North Atlantic.

Since the data reveal a small increase in the yearly mean westward velocity over about 7.5 years, we ask, "What can cause the decrease in flux of the old records?" The answer can be seen in the bottom part of Fig. 10. The bottom data record in Fig. 10 (fastest westward velocity) was from the current meters at $0^{\circ}30'N$ at a depth of 4191 m. This shows a clear downward slope indicating an increase in the westward velocity. The closest comparable current meter in 1992–1994 was at 4100 m depth and it alone was probably responsible for most of the change in the 1992–1994 flux estimate with time. This 1992–1994 record had a big burst of velocity to the west for the first 6 months without such a corresponding large burst during the next year. The other 1992–1994 current meters also showed bursts in speed, but each year they were about the same size. The burst in the 1992–1994 westward current at $0^{\circ}30'N$ and depth 4191 m was big enough to make the early part of the record have annual average velocity almost twice that at the end of the record.

We conclude that this current is an extremely steady long-term flow. For climate changes over decades, deep ocean flows through other gaps might thus show small but very important trends if small changes in their speed can be measured over long times with high precision. Conventional instruments meet the requirements. The most important future task is to locate the pertinent deep gaps.

Acknowledgements

Support was provided by the National Science Foundation, Physical Oceanography Section under Grant OCE98–10607. The Paul M. Fye Chair of the Woods Hole Oceanographic Institution provided support for part of the analysis. We thank Scott E. Worrilow, the late Ryan Schrawder, and Brian Hogue for current meter deployment, and recovery and Craig Marquette

for the mooring design. We also acknowledge with thanks the work of the late Carol Alessi for processing the raw current meter data from 2001 and Marg Zemanovic for processing the 2003 current meter data. Woods Hole Oceanographic Institution Contribution ♯11129.

Appendix A. Tidal constituents

The tidal constituents were calculated using the Matlab program t_tide.m (Pawlowicz et al., 2002). Tables 4–9 give the most energetic constituents of the 6 VACM current meters during 1999–2001.

Table 4
Tidal components for M1-4200

M1	4214 m	Fmaj (cm/s)	Emaj (cm/s)	Fmin (cm/s)	Emin (cm/s)	Finc (cm/s)	Einc (cm/s)	Pha (cm/s)	Epha (cm/s)
Name	Freq								
SA	1.140741E−04	1.365	1.323	0.345	0.669	171.892	27.104	66.800	66.800
SSA	2.281591E−04	0.929	1.197	0.053	0.703	3.457	38.091	104.575	104.575
MSM	1.309781E−03	0.423	0.871	−0.037	0.666	159.675	55.082	146.107	146.107
MM	1.512152E−03	0.736	1.135	−0.034	0.640	174.159	47.252	107.315	107.315
MSF	2.821933E−03	0.392	1.023	0.010	0.594	155.110	58.089	176.935	176.935
MF	3.050092E−03	0.456	0.938	−0.106	0.647	148.738	74.303	171.460	171.460
O1	3.873065E−02	0.441	0.093	−0.072	0.091	147.871	12.198	11.790	11.790
K1	4.178075E−02	0.515	0.093	−0.088	0.099	139.443	11.093	11.213	11.213
M2	8.051140E−02	1.598	0.159	−0.062	0.142	123.976	5.033	5.174	5.174
S2	8.333333E−02	0.717	0.143	−0.105	0.135	116.265	12.612	12.617	12.617

The data columns are the name of the tidal constituent, the frequency, the major axis, the major axis error, the minor axis, the minor axis error, the ellipse inclination, the error in the ellipse inclination, the Greenwich phase, and the error in the Greenwich phase.

Table 5
As in Table 4 except for M1-4300

M1	4314 m	Fmaj (cm/s)	Emaj (cm/s)	Fmin (cm/s)	Emin (cm/s)	Finc (cm/s)	Einc (cm/s)	Pha (cm/s)	Epha (cm/s)
Name	Freq								
SA	1.140741E−04	1.468	1.332	0.064	0.513	10.318	22.608	356.318	50.731
MM	1.512152E−03	0.457	0.794	−0.087	0.481	159.427	47.423	136.612	140.853
O1	3.873065E−02	0.490	0.084	−0.008	0.088	164.446	11.103	149.392	9.101
K1	4.178075E−02	0.536	0.072	−0.008	0.090	154.494	9.784	137.915	9.993
M2	8.051140E−02	1.579	0.156	−0.054	0.112	120.223	5.416	196.350	4.959
S2	8.333333E−02	0.776	0.160	−0.132	0.138	115.796	10.017	239.262	12.953

Table 6
As in Table 4 except for M2-4200

M2	4218 m	Fmaj (cm/s)	Emaj (cm/s)	Fmin (cm/s)	Emin (cm/s)	Finc (cm/s)	Einc (cm/s)	Pha (cm/s)	Epha (cm/s)
Name	Freq								
SA	1.140741E−04	0.640	0.679	0.115	0.812	17.095	97.913	137.154	98.701
SSA	2.281591E−04	0.502	0.676	0.200	0.658	158.740	120.946	294.574	153.988
MSM	1.309781E−03	0.630	0.703	−0.059	0.740	162.438	109.868	209.723	116.647
MM	1.512152E−03	0.646	0.685	−0.236	0.672	34.327	90.528	186.030	99.547
MSF	2.821933E−03	0.427	0.741	−0.173	0.612	81.372	97.175	107.674	125.899
M2	8.051140E−02	1.327	0.138	−0.935	0.142	22.104	17.543	340.995	14.846
S2	8.333333E−02	0.487	0.110	−0.424	0.131	179.601	76.980	220.421	75.758

Table 7
As in Table 4 except for M2-4300

M2	4317 m	Fmaj (cm/s)	Emaj (cm/s)	Fmin (cm/s)	Emin (cm/s)	Finc (cm/s)	Einc (cm/s)	Pha (cm/s)	Epha (cm/s)
Name	Freq								
MSM	1.309781E−03	0.514	0.416	0.221	0.452	15.331	80.562	80.919	88.285
MM	1.512152E−03	0.541	0.446	−0.218	0.457	62.981	70.173	203.474	72.460
MF	3.050092E−03	0.485	0.453	0.001	0.452	81.368	70.350	228.577	79.175
M2	8.051140E−02	1.274	0.143	−1.006	0.169	17.414	25.259	344.894	21.226
S2	8.333333E−02	0.491	0.125	−0.396	0.149	176.638	63.583	226.336	59.231

Table 8
As in Table 4 except for M3-4200

M3	4191 m	Fmaj (cm/s)	Emaj (cm/s)	Fmin (cm/s)	Emin (cm/s)	Finc (cm/s)	Einc (cm/s)	Pha (cm/s)	Epha (cm/s)
Name	Freq								
SA	1.140741E−04	2.300	1.400	−0.117	0.824	169.361	24.114	260.168	39.010
SSA	2.281591E−04	1.040	1.149	−0.450	0.765	1.048	55.438	352.818	91.408
MSM	1.309781E−03	0.455	0.913	0.034	0.873	43.636	74.554	90.711	161.072
MSF	2.821933E−03	0.419	0.918	0.225	0.795	166.792	73.691	81.141	174.524
O1	3.873065E−02	0.432	0.091	−0.037	0.088	141.025	12.717	157.231	12.283
K1	4.178075E−02	0.404	0.083	−0.070	0.079	137.339	14.170	153.010	12.327
M2	8.051140E−02	1.490	0.157	−0.492	0.144	150.606	6.962	202.384	6.437
S2	8.333333E−02	0.452	0.132	−0.035	0.149	141.125	19.345	242.822	18.273

Table 9
As in Table 4 except for M3-4300

M3	4291 m	Fmaj (cm/s)	Emaj (cm/s)	Fmin (cm/s)	Emin (cm/s)	Finc (cm/s)	Einc (cm/s)	Pha (cm/s)	Epha (cm/s)
Name	Freq								
SA	1.140741E−04	1.285	0.756	0.106	0.679	179.289	32.396	215.823	40.665
SSA	2.281591E−04	0.612	0.723	−0.041	0.509	176.552	67.921	85.591	82.240
O1	3.873065E−02	0.464	0.089	−0.044	0.087	128.201	10.577	165.727	12.748
K1	4.178075E−02	0.429	0.086	−0.021	0.090	137.540	10.656	153.205	12.372
M2	8.051140E−02	1.472	0.138	−0.519	0.148	145.382	6.914	204.523	6.684
S2	8.333333E−02	0.487	0.138	−0.027	0.168	139.765	19.307	246.947	16.114

References

Beardsley, R.C., Limeburner, R., Rosenfeld, R.K., 1985. Introduction to CODE-2 moored array and large-scale data report, CODE-2: moored array and large-scale data report. In: Limeburner, R. (Ed.), Woods Hole Oceanographic Institution Technical Report, WHOI-85-35, pp. 1–21.

Coles, V.J., McCartney, M.S., Olson, D.B., Smethie Jr., W.M., 1996. Changes in Antarctic bottom water properties in the western South Atlantic in the late 1980s. Journal of Geophysical Research 101 (C4), 8957–8970.

Dickson, R.M., Brown, J., 1994. The production of North Atlantic deep water: sources, rates and pathways. Journal of Geophysical Research 99, 12319–12341.

Goni, G.J., Trinanes, J.A., 2003. Ocean thermal structure monitoring could aid in the intensity forecast of tropical cyclones. EOS, Transaction of the American Geophysical Union 84 (51), 573–578.

Hall, M., McCartney, M.S., Whitehead, J.A., 1997. Antarctic bottom water flux in the Equatorial Western Atlantic. Journal of Physical Oceanography 27, 1903–1926.

Hansen, B., Turrell, W.R., Osterhus, S., 2001. Decreasing overflow from the Nordic seas into the Atlantic Ocean through the Faroe Bank Channel since 1950. Nature 411, 927–930.

Hogg, N.D., 2001. Quantification of the Deep Circulation. In: Siedler, G., Church, J., Gould, J. (Eds.), Ocean Circulation and Climate. Academic Press, San Diego, CA, pp. 259–270.

Hogg, N.G., Zenk, W., 1997. Long period changes in the bottom water flowing through Vema Channel. Journal of Geophysical Research 102 (C7), 15,639–15,646.

Hogg, N.G., Biscaye, P., Gardner, W., Schmitz Jr., W.J., 1982. On the transport and modification of Antarctic bottom water in the Vema Channel. Journal of Marine Research 40 (Suppl.), 231–263.

Hogg, N.G., Siedler, G., Zenk, W., 1999. Circulation and variability at the southern boundary of the Brazil Basin. Journal of Physical Oceanography 29 (2), 145–157.

Luyten, J., McCartney, M.S., Stommel, H., Dickson, R., Gmitrowicz, E., 1993. On the sources of North Atlantic deep water. Journal of Physical Oceanography 23, 1885–1892.

McCartney, M.S., Curry, R., 1993. Trans-equatorial flow of Antarctic bottom water in the Western Atlantic Ocean: abyssal geostrophy at the equator. Journal of Physical Oceanography 23, 1264–1276.

Mercier, H., Speer, K., 1998. Transport of bottom water in the Romanche Fracture Zone and Chain Fracture Zone. Journal of Physical Oceanography 28, 779–790.

Pawlowicz, R., Beardsley, B., Lentz, S., 2002. Classical tidal harmonic analysis with error analysis in MATLAB using T_TIDE. Computers and Geosciences 28, 929–937.

Rhein, M., Stramma, L., Send, U., 1995. The Atlantic deep western boundary current: water masses and transports near the equator. Journal of Geophysical Research 100 (C2), 2441–2457.

Rhein, M., Stramma, L., Krahmann, G., 1998. The spreading of Antarctic bottom water in the tropical Atlantic. Deep-Sea Research 45, 507–527.

Saunders, P.M., 1990. Cold outflow from the Faeroe Bank Channel. Journal of Physical Oceanography 20, 29–43.

Speer, K.G., Zenk, W., 1993. The flow of Antarctic bottom water into the Brazil Basin. Journal of Physical Oceanography 23, 2667–2682.

Stammer, D., Boning, C.W., 1992. Mesoscale variability in the Atlantic Ocean from Geosat Altimetry and WOCE high-resolution numerical modeling. Journal of Physical Oceanography 22, 732–752.

Warren, B.A., 1981. Deep Circulation of the world ocean. In: Warren, B.A., Wunsch, C. (Eds.), Evolution of Physical Oceanography, Scientific Surveys in honor of H. Stommel. The MIT Press, Cambridge, MA, pp. 6–41.

Whitehead, J.A., 1998. Topographic control of ocean flows in deep passages and straits. Reviews of Geophysics 36, 423–440.

Whitehead, J.A., Worthington, L.V., 1982. The flux and mixing rates of Antarctic bottom water within the North Atlantic. Journal of Geophysical Research 87 (C10), 7903–7924.

Zenk, W., Hogg, N., 1996. Warming trend in Antarctic bottom water flowing into the Brazil Basin. Deep-Sea Research 43 (9), 1461–1473.

Zenk, W., Siedler, G., Lenz, B., Hogg, N.G., 1999. Antarctic bottom water flow through the Hunter Channel. Journal of Physical Oceanography 29 (11), 2785–2801.